AIAA JOURNAL
Vol. 39, No. 7, July 2001

Passive Vibration Suppression of Flexible Space Structures via Optimal Geometric Redesign

Prasanth B. Nair* and Andrew J. Keane†
University of Southampton, Highfield, Southampton, England SO17 1BJ, United Kingdom

A computational framework is presented for the design of large flexible space structures with nonperiodic geometries to achieve passive vibration suppression. The present system combines an approximation model management framework (AMMF) developed for evolutionary optimization algorithms (EAs) with reduced basis approximate dynamic reanalysis techniques. A coevolutionary genetic search strategy is employed to ensure that design changes during the optimization iterations lead to low-rank perturbations of the structural system matrices, for which the reduced basis methods give high-quality approximations. The *k*-means algorithm is employed for cluster analysis of the population of designs to determine design points at which exact analysis should be carried out. The fitness of the designs in an EA generation is then approximated using reduced basis models constructed around the points where exact analysis is carried out. Results are presented for the optimal design of a two-dimensional cantilevered space structure to achieve passive vibration suppression. It is shown that significant vibration isolation of the order of 50 dB over a 100-Hz bandwidth can be achieved. Further, it is demonstrated that the AMMF can potentially arrive at a better design compared to conventional approaches when a constraint is imposed on the computational budget available for optimization.

I. Introduction

DESIGN optimization of large flexible space structures to meet stringent performance specifications is an enabling technology to ensure the cost effectiveness and success of future space missions. For example, Earth science platforms in both low Earth and geostationary orbits require the ability to acquire simultaneous and continuous observation of the Earth with minimum interference, vibrational or otherwise.[1] Integrated controls-structures design procedures utilizing formal optimization techniques have emerged as a rational methodology to design this class of spacecraft, which require precise attitude pointing and vibration suppression. This methodology allows for simultaneous improvement of the controlled system performance in terms of pointing performance and controller energy requirements and also minimization of the payload mass.

The research programs supported by the NASA controls-structures-interaction (CSI) technology program have demonstrated, both analytically and experimentally, the potential benefits of using multidisciplinary design optimization methodology to simultaneously achieve weight savings and improved control system performance of large flexible space structures (for example, see Refs. 2 and 3). These studies mainly approached the design problem by sizing periodic structures and the controller gain parameters to optimize the system performance in the low-frequency region. For a comprehensive exposition of the dynamics and control of flexible space structures, the reader is referred to the monograph edited by Junkins.[4]

Recently, Keane[5] and Keane and Bright[6] have explored different directions, wherein space structures with unusual, that is, nonperiodic or irregular, geometries are designed to achieve passive vibration isolation in the medium-frequency regime. The motivation for this comes from earlier theoretical investigations into the effect of disorder on the vibration transmission characteristics of periodic structures. These studies indicate that the mechanism of constructive interference of energy waves in nonperiodic structures can be exploited to design structures that behave as passive vibration filters. Vibration isolation is achieved here via energy reflection as opposed to dissipation. It has been demonstrated using computational optimization studies that significant vibration isolation can be achieved by departing from conventional periodic structural configurations. The theoretical predictions for the optimized designs were validated by laboratory experiments on model aerospace structures.[6] Theoretical and numerical studies related to the design of near-periodic structures to minimize vibration transmission levels have been presented by Langley[7] and Langley et al.[8]

This design approach holds great potential because significant vibration isolation can be achieved via passive means alone. However, as noted earlier in Ref. 9, the inclusion of geometric design variables leads to a large-scale nonconvex design space, and hence, evolutionary optimization techniques such as genetic algorithms (GAs) are required to ensure convergence to good designs.

It is known that stochastic design space search techniques such as GAs tend to be profligate in terms of the number of function evaluations required to converge to an optimal solution. Hence, such a design methodology is computationally expensive and may require supercomputing power for application to practical structures. Moreover, the repeated evaluation of the dynamic response leads to a considerable increase in the computational cost, especially in the medium-frequency region when large-scale finite element models are used. These characteristics motivate the development of a computational optimization framework for arriving at good designs on a limited computational budget.

This paper focuses on design optimization of large flexible space structures for vibration suppression. A methodology proposed earlier by Keane,[5] which exploits the intrinsic vibration filtering capabilities of nonperiodic structural systems to achieve passive vibration isolation, is the underlying design philosophy used in the present approach. The primary objective of this research is to develop optimization strategies for arriving at good designs on a limited computational budget, that is, using a reduced number of exact analyses.

The approach used here aims to achieve this objective by integrating computationally cheap approximate analysis models with evolutionary optimization algorithms. Two reduced basis methods are used in this research to approximate the dynamic response of modified structural systems. The first formulation seeks to approximate the eigenvalues and eigenvectors, which are then used to compute the frequency response. The second method involves direct approximation of the frequency response via a dynamic stiffness matrix formulation. Both the reduced basis methods use the results of a single exact analysis to approximate the dynamic response. An approximate model management framework (AMMF) is then developed to make use of the computationally cheap approximate analysis techniques in lieu of exact analysis to arrive at better designs

Received 16 March 2000; revision received 15 September 2000; accepted for publication 30 October 2000.

*Ph.D. Student, Computational Engineering and Design Center, School of Engineering Sciences. Member AIAA.

†Professor of Computational Engineering, Director, Computational Engineering and Design Center.

on a limited computational budget. A coevolutionary genetic search strategy is employed to ensure that design changes during the optimization iterations lead to low-rank perturbations of the structural system matrices. This ensures that the reduced basis methods developed give good quality approximations for moderate changes in the geometric design variables. The k-means algorithm is employed for cluster analysis of the population of designs to determine design points at which exact analysis should be carried out. The fitness of the designs in an evolutionary optimization algorithm generation is then approximated using reduced basis models constructed around the points where exact analysis is carried out.

Results are presented for the optimal design of a two-dimensional space structure to achieve passive vibration suppression. It is shown that significant vibration isolation of the order of 50 dB over a 100-Hz bandwidth can be achieved. Further, it is demonstrated that the coevolutionary search strategy can arrive at a better design as compared to conventional approaches, when a constraint is imposed on the computational budget available for optimization. Computational studies are also presented to gain some insights into the mechanisms employed by the optimal design to achieve this performance.

This paper is organized as follows. Section II presents an overview of the background research on dynamics of periodic and disordered structures, Sec. III presents reduced basis methods for dynamic reanalysis of modified structures, Sec. IV proposes an AMMF based on coevolutionary GA that integrates reduced basis methods to enhance the possibility of arriving at good designs on a limited computational budget, Sec. V describes the demonstration example considered, Sec. VI outlines the optimization strategies applied to this problem, Sec. VII summarizes the performance of the various optimization strategies, Sec. VIII presents numerical investigations to gain insights into the mechanisms involved in the vibration transmission characteristics of the best design, and Sec. IX concludes the paper.

II. Background

Many modern aerospace structures are composed of a number of identical substructures that are uniformly connected in a repetitive pattern, for example, stiffened shell structures, turbine assemblies, and large flexible space structures. Such structures tend to have very particular vibration transmission behavior characterized by a series of overlapping passbands and stop-bands (where energy is either transmitted very easily or hardly at all). This behavior has been the focus of much theoretical research, which has concentrated on the performance of perfectly periodic structures (for example, see Mead[10]) and also those with disordered features (for example, see Langley[7]). However, the mean behavior of ensembles of randomly disordered systems can sometimes hide the dramatically different behavior of individual members with unusual properties, that is, some sets of irregularities could result in the ability to block vibration transmission across wide frequency ranges.

One approach to design[7] is to exploit this behavior of periodic structures so that the stopbands span the frequencies of vibration excitation. Theoretical and experimental studies have well demonstrated that, when a structure deviates from ideal periodicity, the vibration transmission characteristics can change dramatically, that is, disorder in periodicity can lead to disruption of the passband and stopband behavior. Hence, the idea of designing periodic structures in this way has not met with much practical success.

Manufacturing uncertainties, structural faults, or changes occurring in service could easily lead to vibration localization, which causes the response to be confined to a few segments of the structure as opposed to a response that extends throughout the structure. As discussed by Lust et al.,[11] disorder in the periodicity may also induce perturbations in a mode shape, which leads to an increase in the participation of that mode in the response. Hence, depending on the disorder pattern, localization could be catastrophic because excessive vibration levels could cause structural failure or destabilizing CSIs.[12] An earlier study by Benedikssen[13] has shown that localization is most likely to occur in space structures that have high modal density and many weakly coupled substructures.

On the other hand, localization could be beneficial because it could potentially be harnessed as a passive vibration isolation mechanism. The numerical studies presented in Ref. 11 indicate that small random disorder could lead to as much as three orders reduction in the forced vibration response across a narrow-frequency bandwidth of 2 Hz. Numerical studies conducted by Keane and Manohar[14] and Langley et al.[8] have shown that, when only a single frequency dominates the response, a near-periodic structure (a periodic structure with small disorder) can achieve a dramatic reduction in the response level at that frequency. This is primarily because of the disorder causing localization of the mode shape under consideration.

However, to design structures that act as passive vibration filters across a broad-frequency bandwidth, larger magnitudes of disorder may be required to achieve similar reductions in the vibration levels. Furthermore, because many modes contribute to the response in a broadband-frequency region, it becomes impossible to arrive at general design rules for achieving reduction in the vibration levels. This is the fundamental premise of the design approach developed by Keane,[5] where a formal optimization technique was used to determine the magnitude and precise nature of disorder that enables a structure to filter vibrations across a 100-Hz bandwidth.

This idea of intentionally designing disorder into periodic structures to reduce vibration levels has also been recently examined by Castanier and Pierre[15] for turbomachinery rotors. It was shown that intentional mistuning can greatly reduce the rotor's sensitivity to random mistuning. These results suggest that nonperiodic structures may be more robust as compared to their periodic counterparts.

III. Approximate Dynamic Reanalysis

The equations of motion in the frequency domain of a linear structural system can be written in the form

$$[\boldsymbol{D}^0(\omega)]\{\boldsymbol{X}^0(\omega)\} = \{\boldsymbol{F}\} \tag{1}$$

where $[\boldsymbol{D}^0(\omega)] = ([\boldsymbol{K}^0] - \omega^2[\boldsymbol{M}^0] + i\omega[\boldsymbol{C}^0]) \in \mathbb{C}^{n\times n}$ is the dynamic stiffness matrix of the structure; $[\boldsymbol{K}^0]$, $[\boldsymbol{M}^0]$, and $[\boldsymbol{C}^0] \in \mathbb{R}^{n\times n}$ are the structural stiffness, mass, and damping matrices, respectively; $\{\boldsymbol{F}\} \in \mathbb{R}^n$ is the amplitude vector of the external harmonic forces; $\{\boldsymbol{X}^0(\omega)\} \in \mathbb{C}^n$ is the displacement response at the excitation frequency ω; n is the total number of degrees of freedom (DOF); and $i = \sqrt{-1}$.

Let $[\Phi^0] \in \mathbb{R}^{n\times m}$ and $[\Lambda^0] \in \mathbb{R}^{m\times m}$ be the modal and diagonal spectral matrices, respectively, of the baseline structure, where m is the number of eigenmodes used to approximate the dynamic response. The eigenvectors are normalized to satisfy the biorthonormality relationships $[\Phi^0]^T[\boldsymbol{M}^0][\Phi^0] = \boldsymbol{I}_m$ and $[\Phi^0]^T[\boldsymbol{K}^0][\Phi^0] = [\Lambda^0]$. Structural damping is assumed to be proportional, that is, $[\boldsymbol{C}^0] = \alpha[\boldsymbol{K}^0] + \beta[\boldsymbol{M}^0]$, where $\boldsymbol{I}_m \in \mathbb{R}^{m\times m}$ is the identity matrix.

Transformation of Eq. (1) to modal coordinates gives

$$\left([\Lambda^0] - \omega^2\boldsymbol{I}_m + i\omega\left[\boldsymbol{C}_q^0\right]\right)\{\boldsymbol{q}^0(\omega)\} = \left\{\boldsymbol{F}_q^0\right\} \tag{2}$$

where $\{\boldsymbol{q}^0(\omega)\} \in \mathbb{C}^m$ is the vector of modal participation factors at the excitation frequency ω, $[\boldsymbol{C}_q^0] = [\Phi^0]^T[\boldsymbol{C}^0][\Phi^0] \in \mathbb{R}^{m\times m}$ is the diagonal modal damping matrix, and $\{\boldsymbol{F}_q^0\} = [\Phi^0]^T\{\boldsymbol{F}\} \in \mathbb{R}^m$.

Now, consider the case when changes in the structural parameters lead to perturbations $[\Delta\boldsymbol{K}]$, $[\Delta\boldsymbol{M}]$, and $[\Delta\boldsymbol{C}]$ in the stiffness, mass, and damping matrices, respectively. The equations of motion of the perturbed system can then be written as

$$([\boldsymbol{D}^0(\omega)] + [\Delta\boldsymbol{D}(\omega)])\{\boldsymbol{X}(\omega)\} = \{\boldsymbol{F}\} \tag{3}$$

where $[\Delta\boldsymbol{D}(\omega)] = [\Delta\boldsymbol{K}] - \omega^2[\Delta\boldsymbol{M}] + i\omega[\Delta\boldsymbol{C}]$ is the perturbation in the dynamic stiffness matrix.

Here two reduced basis approximation methods are used to reduce the computational burden of numerical optimization using large-scale finite element models (see Ref. 16 by Noor for an overview of reduced basis methods). The first formulation to be presented involves approximating the eigenvalues and eigenvectors of the perturbed eigenvalue problem, which are then used to compute the frequency response. The second formulation is developed for directly approximating the frequency response of modified structures.

A. Modal Reduced Basis Approximation Method

The method used for approximating the eigenvalues and eigenvectors of modified structures was developed earlier in Refs. 17 and 18. This method uses the baseline eigenvector and its first-order approximation term as basis vectors for Ritz analysis for the modified eigenvalue problem. This method is henceforth referred to as the modal reduced basis approximation (MRBA) method.

The MRBA method postulates a reduced basis approximation for the eigenvector of mode i of the perturbed system as $\hat{\boldsymbol{\phi}}_i = \zeta_1 \boldsymbol{\phi}_i^0 + \zeta_2 \Delta\boldsymbol{\phi}_i$, where $\boldsymbol{\phi}_i^0$ is the eigenvector corresponding to the baseline stiffness and mass matrices, $[\boldsymbol{K}^0]$ and $[\boldsymbol{M}^0]$, and $\Delta\boldsymbol{\phi}_i$ is the first-order approximation for the eigenvector perturbation. The coefficients in the reduced basis representation ζ_1 and ζ_2 can be computed by solving the 2×2 eigenproblem

$$\left[\boldsymbol{K}_T^i\right]\{\mathrm{Z}\}^i = \lambda_i \left[\boldsymbol{M}_T^i\right]\{\mathrm{Z}\}^i \tag{4}$$

where

$$\left[\boldsymbol{K}_T^i\right] = \left[\boldsymbol{\phi}_i^0, \Delta\boldsymbol{\phi}_i\right]^T \{[\boldsymbol{K}] + [\Delta\boldsymbol{K}]\}\left[\boldsymbol{\phi}_i^0, \Delta\boldsymbol{\phi}_i\right] \in \mathbb{R}^{2\times 2} \tag{5}$$

$$\left[\boldsymbol{M}_T^i\right] = \left[\boldsymbol{\phi}_i^0, \Delta\boldsymbol{\phi}_i\right]^T \{[\boldsymbol{M}] + [\Delta\boldsymbol{M}]\}\left[\boldsymbol{\phi}_i^0, \Delta\boldsymbol{\phi}_i\right] \in \mathbb{R}^{2\times 2} \tag{6}$$

Solution of Eq. (4) leads to two possible values for the approximate eigenvalue of mode i and the coefficients of the reduced basis $\{Z\}^T = \{\zeta_1 \zeta_2\}$. Clearly, for the fundamental mode, the value with lowest magnitude gives the best approximation. For the higher modes, the eigenvalue of Eq. (4) that is closest to the higher-order eigenvalue perturbation derived by Eldred et al.[19] is chosen as the best approximation for that mode. The expression for the higher-order eigenvalue perturbation[20] is

$$\hat{\lambda}_i = \lambda_i^0 + \frac{\boldsymbol{\phi}_i^{0T}\left(\Delta\boldsymbol{K} - \lambda_i^0 \Delta\boldsymbol{M}\right)\left(\boldsymbol{\phi}_i^0 + \Delta\boldsymbol{\phi}_i\right)}{\boldsymbol{\phi}_i^{0T}(\boldsymbol{M}^0 + \Delta\boldsymbol{M})\left(\boldsymbol{\phi}_i^0 + \Delta\boldsymbol{\phi}_i\right)} \tag{7}$$

where λ_i^0 is the eigenvalue of mode i for the baseline structure.

After the best approximation for the eigenvalue has been chosen, the corresponding eigenvector approximation can be readily computed. It has been shown by Nair et al.[17] that this method gives good-quality results for moderate to large magnitudes of perturbation in the system matrices. In particular, high-quality approximations can be obtained for low-rank perturbations in the stiffness and mass matrices.

There exists a wealth of methods in the literature for computing first-order approximations of the eigenvectors of perturbed linear algebraic eigenvalue problems (for example, see Refs. 21 and 22). In the present research, a zero-order technique based on the family of modal methods introduced by Akgun[22] is used to compute directly a first-order approximation of the eigenvector perturbation, that is, $\Delta\boldsymbol{\phi}$.

B. Direct Frequency-Response Approximation Methods

The objective of this formulation is to directly approximate the frequency response using a reduced basis. This formulation is henceforth referred to as the direct frequency-response approximation (DFRA) method. The choice of basis vectors used here is motivated by the reduced basis method presented earlier by Kirsch[23] for static reanalysis of structural systems.

In the present formulation, the terms of the Neumann expansion scheme are used as basis vectors to approximate the displacement response of the modified structure. The Neumann expansion for the solution of Eq. (3) can be written as

$$\{\tilde{\boldsymbol{X}}(\omega)\} = \sum_{j=1}^{\infty} (-1)^{j-1} ([\boldsymbol{D}^0(\omega)]^{-1}[\Delta\boldsymbol{D}(\omega)])^{j-1} [\boldsymbol{D}^0(\omega)]^{-1}\{\boldsymbol{F}\} \tag{8}$$

The Neumann expansion series is convergent only when $\|[\boldsymbol{D}^0(\omega)]^{-1}[\Delta\boldsymbol{D}(\omega)]\| < 1$, that is, when the perturbations in the dynamic stiffness matrix are small.

The present formulation uses the terms of Eq. (8) as basis vectors for approximating $\{\boldsymbol{X}(\omega)\}$. The basic premise of this formulation is that the terms of the Neumann expansion, although erroneous in magnitude for large perturbations, provide a good subspace for approximating the perturbed displacement response. Consider the case when p basis vectors are used to approximate the dynamic response. A reduced basis approximation for the displacement response of the perturbed system at a given excitation frequency ω can then be written as

$$\hat{\boldsymbol{X}}(\omega) = \gamma_1(\omega)\{\psi_1(\omega)\} + \gamma_2(\omega)\{\psi_2(\omega)\} + \cdots + \gamma_p(\omega)\{\psi_p(\omega)\} \tag{9}$$

where $\gamma_1(\omega), \gamma_2(\omega), \ldots, \gamma_p(\omega)$ are the undetermined scalars in the reduced basis representation. The basis vectors $\{\psi_1(\omega)\}, \{\psi_2(\omega)\}, \ldots, \{\psi_p(\omega)\} \in \mathbb{C}^n$ in the preceding equation can be written as

$$\{\psi_1(\omega)\} = \{\boldsymbol{X}^0(\omega)\}$$

$$\{\psi_2(\omega)\} = [\boldsymbol{B}(\omega)]\{\psi_1(\omega)\}, \ldots, \{\psi_p(\omega)\} = [\boldsymbol{B}(\omega)]\{\psi_{p-1}(\omega)\} \tag{10}$$

where $[\boldsymbol{B}(\omega)] = [\boldsymbol{D}^0(\omega)]^{-1}[\Delta\boldsymbol{D}(\omega)] \in \mathbb{C}^{n\times n}$. Equation (9) can be written using matrix notation as

$$\{\hat{\boldsymbol{X}}(\omega)\} = [\Psi(\omega)]\{\Gamma(\omega)\} \tag{11}$$

where $[\Psi(\omega)] = [\{\psi_1(\omega)\}, \{\psi_2(\omega)\}, \ldots, \{\psi_p(\omega)\}] \in \mathbb{C}^{n\times p}$ is the matrix of complex basis vectors and $\{\Gamma(\omega)\} = \{\gamma_1(\omega), \gamma_2(\omega), \ldots, \gamma_p(\omega)\}^T \in \mathbb{C}^p$ is the vector of complex undetermined scalars.

The vector of undetermined scalars are computed using a Bubnov–Galerkin scheme. This involves orthogonalization of the residual error in satisfying Eq. (3) to the matrix of basis vectors. Hence, when Eqs. (3) and (11) are used, a reduced-order system of equations to be solved for $\{\Gamma(\omega)\}$ can be written as

$$\left(\left[\boldsymbol{D}_R^0(\omega)\right] + [\Delta\boldsymbol{D}_R(\omega)]\right)\{\Gamma(\omega)\} = \{\boldsymbol{F}_R(\omega)\} \tag{12}$$

where $[\boldsymbol{D}_R^0(\omega)] = [\Psi(\omega)]^H[\boldsymbol{D}^0(\omega)][\Psi(\omega)]$ and $[\Delta\boldsymbol{D}_R(\omega)] = [\Psi(\omega)]^H[\Delta\boldsymbol{D}(\omega)][\Psi(\omega)] \in \mathbb{C}^{p\times p}$ are the reduced baseline dynamic stiffness matrix and the perturbation matrix, respectively, and $\{\boldsymbol{F}_R(\omega)\} = [\Psi(\omega)]^H\{\boldsymbol{F}\} \in \mathbb{C}^p$. The superscript H is the conjugate transpose of a matrix.

Note that the dimension of the reduced complex matrix system of equations is $p \times p$. The solution of Eq. (12) at each excitation frequency of interest gives the vector of complex undetermined constants $\{\Gamma(\omega)\}$. This is then substituted in Eq. (11) to compute the approximate frequency response of the modified structure. The order of the reduced basis approximation is considered here to be equal to $p - 1$, where p is the number of basis vectors used in Eq. (11). When a small number of basis vectors is used in the reduced basis representation, Eq. (12) can be solved in a computationally efficient fashion. The most computationally intensive part of the formulation involves the computation of the basis vectors [see Eq. (10)] and the reduced dynamic stiffness matrices in Eq. (12).

It can be observed from Eq. (10) that the basis vectors can be computed in a recursive fashion. The system of equations to be solved for the jth basis vector can be written as

$$[\boldsymbol{D}^0(\omega)]\{\psi_j(\omega)\} = [\Delta\boldsymbol{D}(\omega)]\{\psi_{j-1}(\omega)\} \tag{13}$$

In Ref. 23 by Kirsch, the terms of the Neumann expansion were computed exactly. However, here, for the sake of computational efficiency, the basis vectors are approximately calculated. Note that the solution of Eq. (13) would require the inversion of $[\boldsymbol{D}^0(\omega)]$. However, the inverse of this matrix is not readily available from the analysis of the baseline structure. To circumvent this, an approximate procedure is used to solve the preceding equation. It can be seen that the solution of Eq. (13) is equivalent to computing the response of the baseline structure to a harmonic excitation with complex magnitude $[\Delta\boldsymbol{D}(\omega)]\{\psi_{j-1}(\omega)\}$. An approximate solution is sought to Eq. (13) in the subspace spanned by the eigenvectors of the baseline structure as

$$\{\psi_j(\omega)\} = [\Phi^0]\{\boldsymbol{b}(\omega)\} \tag{14}$$

where $\{\boldsymbol{b}(\omega)\} \in \mathbb{C}^m$ is the vector of undetermined contributions from each eigenvector to $\{\psi_j(\omega)\}$. When Eqs. (13) and (14) are used, the vector $\{\boldsymbol{b}(\omega)\}$ can be computed by solving

$$\left([\Lambda^0] - \omega^2 \boldsymbol{I} + i\omega\left[\boldsymbol{C}_q^0\right]\right)\{\boldsymbol{b}(\omega)\} = \{\boldsymbol{d}_q(\omega)\} \tag{15}$$

where $\{\boldsymbol{d}_q\} = [\Phi^0]^T[\Delta \boldsymbol{D}(\omega)]\{\psi_{j-1}(\omega)\} \in \mathbb{C}^m$.

Because the coefficient matrix in the preceding equation is diagonal, $\{\psi_j(\omega)\}$ can be efficiently computed using Eqs. (14) and (15). Similarly, all of the basis vectors used in the reduced basis representation of the perturbed displacement response can be efficiently computed. This involves starting with the first basis vector $\{\psi_1(\omega)\} = \{\boldsymbol{X}^0(\omega)\}$ and using Eqs. (14) and (15) to compute the subsequent basis vectors.

Note that the basis vectors computed in such as fashion are approximate in nature. However, the accuracy of the basis vectors can be readily improved by increasing the number of baseline eigenvectors. Alternatively, modal acceleration techniques of the form presented by Akgun[22] can be used to improve the rate of convergence. However, in the present research, only a subset of the baseline eigenvectors is used to approximate the basis vectors. For a detailed comparison study between the accuracy of the MRBA and DFRA methods, the reader is referred to the work by Nair.[24]

IV. AMMF

For large-scale systems, the computational cost of approximate analysis is generally a fraction of that required for exact analysis. Hence, the approximation model can be used in lieu of the exact model during the optimization iterations at a considerably lower computational cost. The underlying idea of the design framework developed here is to use the approximation model for efficiently sampling larger regions of the design space. This is expected to enhance the possibility of obtaining superior designs on a limited computational budget.

The AMMF used here is based on the framework introduced by Nair et al.[25] for integrating general single-point approximation models with evolutionary optimization procedures. The reader is referred to the work of Hajela[26] for a recent review of the state of the art in evolutionary optimization.

The main component of the present AMMF involves the procedure used for the selection of anchor points at which exact analysis is carried out. The baseline eigenparameters computed at the anchor point can then be used to approximate the dynamic-response data at other design points using the reduced basis methods described earlier. In general, approximation errors will increase as the new design point moves away from the anchor point. Because evolutionary optimization algorithms make use of a population of designs and stochastic search operators, the design points in a generation may span the entire design space, that is, the control of step size in the design changes is not a straightforward task as compared to line-search-based optimization algorithms. Hence, advanced strategies are required to ensure that the errors involved in approximate fitness evaluations are controlled to enhance the capability to predict design improvements.

A useful way to control the approximation error is to use a domain decomposition strategy for grouping the design points in a generation into clusters. The k-means algorithm[20] is used here for cluster analysis of the population of designs in a given generation. The anchor point is chosen as the mean vector of the individuals in a cluster. Exact analysis is carried out for this anchor point, and the dynamic response of the other designs in the cluster are approximated based on the results of this exact analysis. The fitness of all of the designs in the population is approximated using this procedure. Note that this step also allows for the possibility of efficient parallelization of the AMMF because the fitness evaluations for designs in each cluster can be carried out concurrently.

As discussed in Ref. 24, an AMMF based on single-species GA does not perform well for problems where a low-fidelity model is used for fitness approximations. This was primarily attributed to the large magnitude of approximation errors that result when all of the design variables are simultaneously perturbed. These errors are quite high, and so make the approximate fitness predictions useless for the purposes of optimization. To reduce the approximation error, a large number of anchor points/clusters are required. However, the computational cost increases substantially with increase in the number of anchor points at which exact analysis is carried out. Fortunately, as observed in earlier studies (for example, see Refs. 17 and 23), the approximation errors are lower when the reduced basis methods are applied to problems involving low-rank perturbations in the system matrices.

To exploit this characteristic of the reduced basis methods, a coevolutionary genetic algorithm (CGA) is employed here in conjunction with the AMMF. A CGA by construction varies only a subset of the design variables at a time. Hence, the design changes during the optimization iterations lead to low-rank perturbations in the system matrices.

A CGA models an ecosystem consisting of two or more sympatric species having an ecological relationship of mutualism. The reader is referred to Ref. 27 by Potter for a detailed overview of CGAs. In the context of structural optimization, the design variables are grouped into sets corresponding to each substructure, that is, each species contain a population of alternative values for the substructure design variables. Collaboration between the various species involves selection of representative values from all of the species and combining them into a vector that is then used to compute the objective function. An individual in a species is, hence, rewarded based on how well it maximizes the objective function within the context of the representatives selected from the other species.

The proposed AMMF for CGA-based search in which the cluster analysis strategy is integrated with the canonical CGA is summarized as follows:

1) Initialize a population of individuals for each species randomly (note that all variables not controlled by this species are left at their original values).

2) Evaluate the fitness of the members of each species. Fitness evaluation involves the use of the following algorithm:

a) Choose representatives from all of the other species.

b) Decompose the design subspace into clusters using the k-means algorithm and compute the anchor point for each cluster. Augment the anchor design vector with the values of the representative designs from other species. Do exact analysis for each anchor point and construct an approximation model around this point.

c) FOR each individual i in a species being evaluated DO

Form collaboration between i and representatives from other species to form the design vector.

Approximate the fitness of collaboration using the approximation model constructed at the anchor point closest to i.

Assign fitness of collaboration to i.

ENDDO

d) Evaluate the best design as predicted by the approximation model using exact analysis. If the exact fitness is greater than that of the best design so far (if it exists), replace the elite individual of this species with the new design.

3) If the termination criteria are not met, then apply a canonical GA involving the operators of reproduction and genetic recombination to arrive at a new population for each species. Go to step 2.

If n_{clus} clusters are used for predicting the fitness of m species, the total number of exact analysis at each generation of the CGA is $mn_{\text{clus}} + m$. The first term is due to the requirement of carrying out exact analysis at the cluster centers for each species. The second term results from exact analysis of the best design in each species (as predicted by the approximation model) to implement elitism and prevent loss of the best design to date. Elitism is implemented here to prevent loss of the fittest design in each species due to both the stochastic nature of the search operators, and the dynamic nature of the fitness evaluation scheme. The best/elite design in a species is chosen as its representative.

In the present design framework, the CGA is allocated the task of finding design improvements in the face of uncertainty in fitness predictions. Moreover, because each species independently coevolves a subset of the design variables, effective collaboration between the species is of crucial importance. Each species must constantly adapt just to remain in parity with the others. Hence, the evolution of each species is constantly driven by evolutionary changes in the species it interacts with as well as the dynamics of the fitness evaluation

scheme. However, the effect of fitness uncertainties on the convergence behavior of CGAs is a subject area that is not yet fully investigated. Preliminary investigations by Potter[27] appear to indicate that CGAs are more sensitive to noise as compared to a single-species GA. Even so, they appear to work well for the present problem.

V. Demonstration Example

The design methodology developed in this research is applied to optimization of the two-dimensional cantilevered structure shown in Fig. 1. The structure is subjected to transverse excitation at joint F near the fixed end. The following values are used for the physical properties of each structural beam member: flexural rigidity $EI = 1.286 \times 10^3$ Nm^2, axial rigidity $EA = 6.987 \times 10^6$ N, and mass per unit length $m = 2.74$ kg/m. The length of the structural members is either 1 m or 1.414 m. A finite element (FE) model for this structure is developed using Euler–Bernoulli beam theory and a consistent mass matrix formulation. A proportional damping model of the form $\boldsymbol{C} = \alpha \boldsymbol{K} + \beta \boldsymbol{M}$ is chosen, where $\alpha = 0.0$ and $\beta = 20.0$ to reflect a lightly, mass proportional, damped structure.

The objective of the design problem considered here is to suppress the vibration response at joint R over the frequency region of 100–200 Hz. This design problem simulates the case where a given point on a space structure must be isolated from external disturbances. For example, an instrumentation package may be mounted at joint R, and it is desired to isolate it from external vibrations arising in the main body of the satellite.

The objective function for this design problem is defined as the integral of the frequency responses at joint R from 100 to 200 Hz. The performance measure of a candidate design is, therefore, defined as

$$\boldsymbol{J} = -20 \log_{10} \left\{ \frac{1}{I_0} \int_{100}^{200} [u_R(\omega) + v_R(\omega) + L\theta_R(\omega)] \, \mathrm{d}\omega \right\} \quad (16)$$

where u_R, v_R, and θ_R are the axial, transverse, and rotational components of the displacement response at joint R, respectively. I_0 is the integral of the frequency responses at R for the baseline periodic structure shown in Fig. 1.

The first 100 modes are used to compute the dynamic response of the structure in the region of 100–200 Hz. The integral in Eq. (16) is evaluated using a 35-point integration rule, that is, the response is computed at a resolution of around 2.7 Hz. The design is parameterized in terms of the coordinates of the structural joints, which are allowed to vary between ± 0.25 m from the baseline values, with the coordinates of joint R being kept fixed. This leads to a total of 40 geometric design variables.

A FE model with 5 elements per structural member, that is, 567 DOF, is used to compute the free-vibration natural frequencies and mode shapes of the structure. For this problem size, the exact analysis method takes an average of 152 s to compute the objective function. In comparison, the MRBA method takes 2.2 s, with the DFRA1 and DFRA2 methods [i.e., DFRA methods of order one and two, respectively, corresponding to $p = 2$ and $p = 3$ in Eq. (9)] taking 7.5 and 9.1 s, respectively. The numerical studies reported here were conducted on a Silicon Graphics Origin 2000 machine with R10,000 processors.

VI. Optimization Strategies

A. Conventional GA

For the conventional GA approach, an elitist GA implementation with binary tournament selection, uniform crossover, and bit mutation is used. The GA implementation used here is typical of that described by Goldberg.[28] The probability of crossover and bit mutation are kept constant at 0.5 and 0.01, respectively. A binary string of 10 bits is used to represent each of the design variables. A population size of 100 is used for all of the runs. Note that this approach uses the exact analysis model to compute the objective function throughout the search. The conventional GA was terminated after 30 generations, that is, around 125 h of wall time or 3000 exact analysis. Four runs were carried out with different initial populations for statistical analysis of the performance of this search strategy.

B. CGA–AMMF Approach

In the coevolutionary search strategy applied to this problem, the structural design variables are decomposed into five sets of eight variables each. Each set corresponds to the coordinates of the four joints within two bays of the structure. Five species are set up, which are to control each set of design variables.

A population size of 20 is used for each species. Uniform crossover and bit mutation are applied at a probability of 0.5 and 0.01, respectively. A binary tournament selection operator was used throughout the search. For each species, the design space is decomposed at each generation into two clusters for computing the anchor points. Exact analysis is carried out at the center of the cluster, and the fitness of the designs within each cluster is approximated using a reduced basis model constructed around the anchor point. To implement elitism, an additional exact analysis is carried out for the best design within each species, that is, a total of 3 exact and 20 approximate analysis are carried out for each species in a generation. In summary, the conventional GA approach uses 100 exact analysis at each generation, whereas the CGA–AMMF approach uses 15 exact analysis and 100 approximate analysis at each ecosystem generation.

The CGA–AMMF is used in conjunction with the three approximation methods considered here, that is, the MRBA, DFRA1, and DFRA2 methods. For each case, four runs were carried out to compute the statistics of the convergence trends. The termination criterion was chosen as 125 h of wall time (or 150 ecosystem generations if this was reached sooner).

C. Broyden–Fletcher–Goldfarb–Shanno Algorithm

A limited-memory Broyden–Fletcher–Goldfarb–Shanno (BFGS) algorithm developed by Zhu et al.[29] for bound constrained optimization problems has also been applied to this example problem. The BFGS method used the exact analysis model throughout to evaluate the objective function and its gradients. The gradients were computed using forward finite differences with a step size of 1.0×10^{-5}. Similar to the conventional GA approach, the termination criterion was chosen to be 125 h of wall clock time, that is, around 3000 exact analyses. The baseline periodic structure shown in Fig. 1 was used as the initial design.

VII. Results and Discussion

A. Comparison of Convergence Trends

As described earlier, a total of five optimization strategies were applied to the design problem: 1) conventional GA, 2) CGA–AMMF with MRBA method, 3) CGA–AMMF with DFRA1 method, 4) CGA–AMMF with DFRA2 method, and 5) BFGS method. Note that the convergence trends for the first four strategies are averaged over four runs. Each run for an optimization strategy took around 5 days of computer time on a single processor.

The averaged convergence trends of the five optimization strategies as a function of wall time and number of exact analysis are shown in Figs. 2 and 3. A statistical analysis of the performance of the optimization strategies is summarized in Table 1. The following observations can be made from these results.

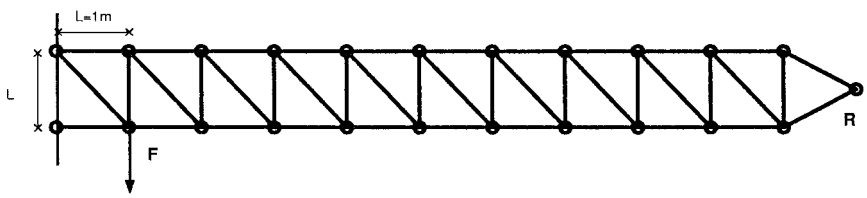

Fig. 1 Two-dimensional space structure.

1) As compared to the DFRA methods, the MRBA method shows a much slower convergence rate. On average, after around 60 h of wall time, this strategy shows worse performance as compared to the conventional GA. Note that this strategy used a total of 2250 exact analyses and 15,000 approximate calculations within the termination criterion used. This suggests that most of the time, the approximations obtained using the MRBA method were not very useful for predicting design improvements. However, this strategy gives better results than the BFGS method. The best design obtained using this strategy has an objective function value of around 36 dB.

Table 1 Statistics of optimal design obtained using various optimization approaches

Optimization approach	Mean	Standard deviation	Best value	Worst value
Conventional GA	37.85	2.06	40.67	36.01
CGA–AMMF + MRBA	33.33	2.61	35.81	29.72
CGA–AMMF + DFRA1	40.01	4.62	46.07	36.75
CGA–AMMF + DFRA2	47.44	1.24	49.74	46.31
BFGS	——	——	27.52	——

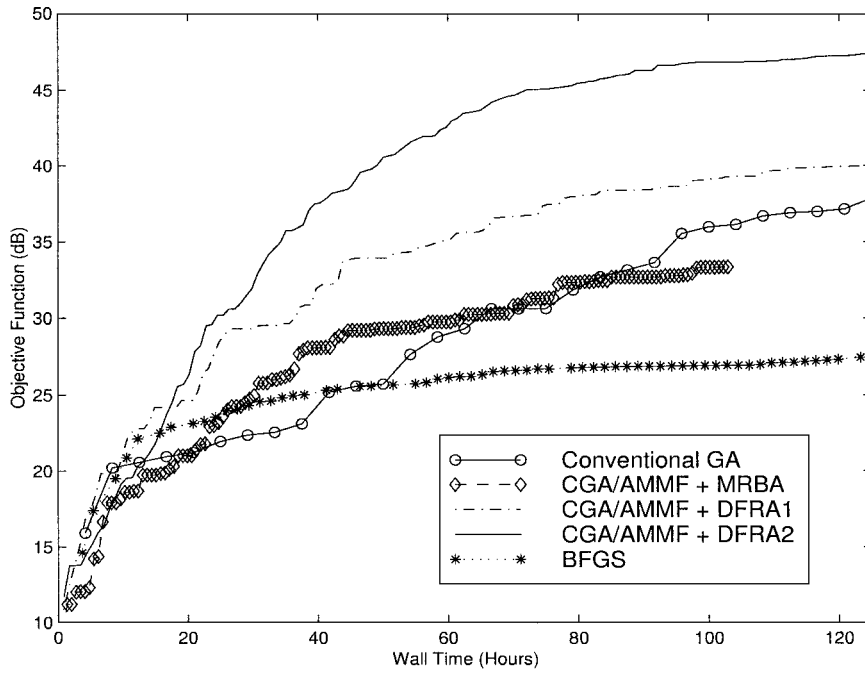

Fig. 2 Comparison of optimization history as a function of computational time for all of the optimization approaches.

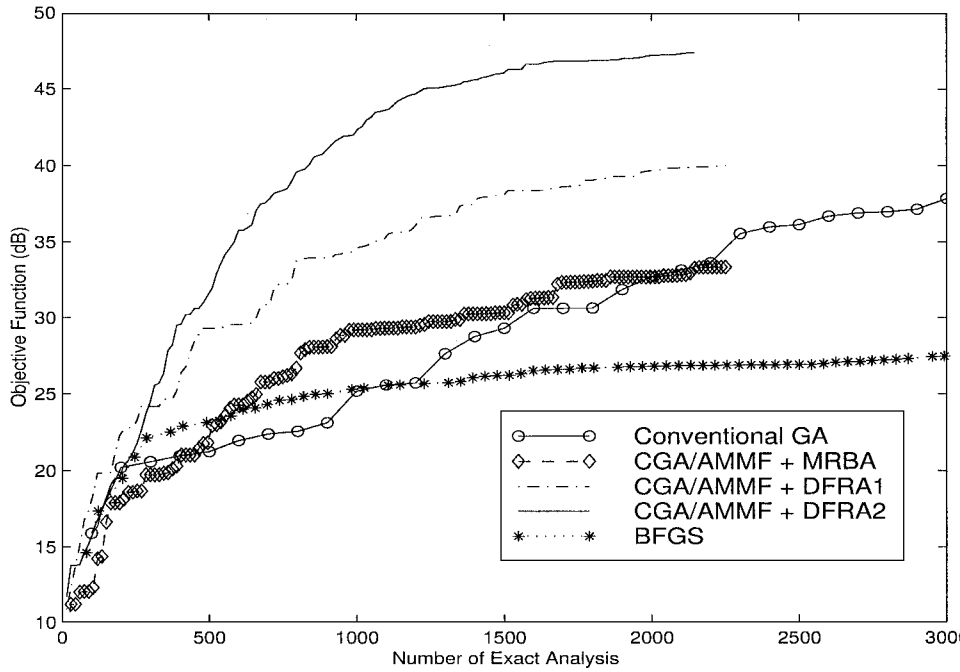

Fig. 3 Comparison of optimization history as a function of the number of exact analysis for all of the optimization approaches.

2) The BFGS method has a rapid convergence rate in the first 15 h. However, thereafter convergence is rather slow. Numerical experiments using other values for the finite difference step size did not improve the performance of this algorithm. It appears that the algorithm gets entrapped in a local optimum during the iterations and, hence, converged toward a suboptimal design as compared to the other strategies.

3) The results clearly indicate that, over the time budget allocated for optimization, the CGA–AMMF strategy combined with the DFRA methods gives better results as compared to the other strategies. Over the time window of 0–18 h, the DFRA1 method gives the best design. After this time window, the DFRA2 method gives significantly better designs on average throughout. Note, from Table 1, that the performance of the DFRA2-based optimization strategy is significantly better than all of the other strategies with regards to all of the statistical measures considered. The best design obtained using this method shows significant vibration isolation of around 50 dB.

4) The quality of approximations appears to be a fundamental characteristic influencing the convergence trends reported here. Note that the MRBA method is around three times faster than the DFRA1 and DFRA2 methods. However, the high quality of the approximations obtained using the DFRA methods appear to be much more useful when predicting the effect of geometry modifications on the objective function.

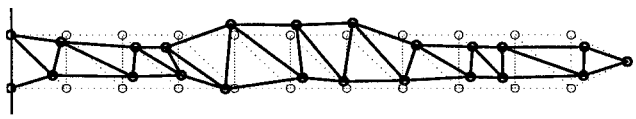

Fig. 4 Optimized structure using conventional GA: objective function, 41 dB; and volume ratio, 0.92.

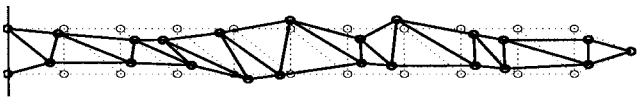

Fig. 5 Optimized structure using CGA–AMMF approach with DFRA2 method: objective function, 50 dB; and volume ratio, 0.94.

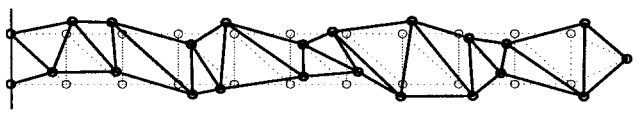

Fig. 6 Optimized structure using BFGS algorithm: objective function, 26 dB; and volume ratio, 1.05.

B. Comparison of Optimal Geometry and Response

The configurations of the optimal designs obtained using some of the various optimization strategies are shown in Figs. 4–6. For the evolutionary optimization approaches, the optimized structures shown in Figs. 4–6 are the best designs obtained over four independent runs with different initial populations. The corresponding objective function values for all of the designs are also shown in Figs. 4–6. Also noted is the ratio of the structural weight of the optimum design to that of the baseline structure (referred to as volume ratio in Figs. 4–6).

It can be seen that the optimal geometry shown in Figs. 4 and 5 have some similarities. The best design of all, shown in Fig. 5, with the objective function value of 50 dB has a quite regular geometry near the base and the tip. However, the middle portion of the structure has a rather unusual geometry. The optimal design found using the BFGS algorithm has the worst vibration isolation performance as compared to the other designs. Not surprisingly, the geometry of this suboptimal design (see Fig. 6) is significantly different as compared to the other designs.

Also note that most of the designs have lower structural weight as compared to the baseline structure. In particular, the structural weight of the best design shown in Fig. 5 is around 6% lower. Recollect that no constraints were imposed on the structural weight in the optimization formulation. This suggests that it is possible to simultaneously decrease the structural weight and significantly improve the vibration filtering characteristics of the structure considered here. Note also, however, that no constraints have been placed on the static strength here.

Figure 7 compares the total displacement level at joint R for the optimum designs in Figs. 4–6. The response of the baseline structure is shown in Figs. 4–6 for comparison. It can be seen that the optimum design obtained using the CGA–AMMF with the DFRA2 method show significant reductions in the response over the 100-Hz frequency band region of interest. In addition, vibration isolation of the order of 24 dB over the broadband-frequency region of 0–200 Hz is achieved. Clearly, improvement in the performance is not achieved at the expense of increased response at frequencies that are not considered in the optimization formulation.

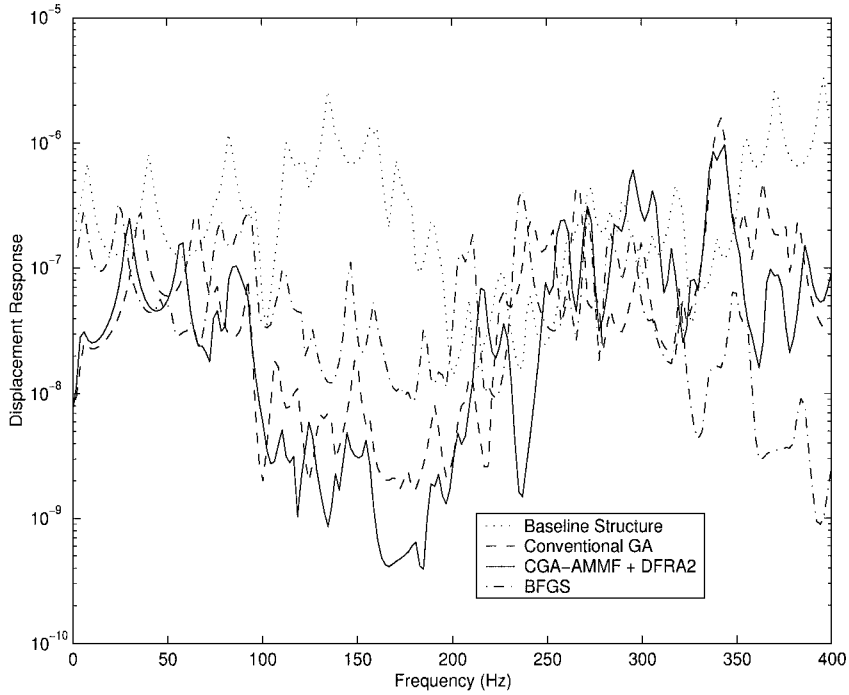

Fig. 7 Comparison of total displacement levels at R for the optimal designs using conventional GA, BFGS algorithm, and CGA–AMMF with DFRA2 method.

VIII. Response Characteristics of Optimized Design

Recollect that the best design (see Fig. 5) shows around 50-dB vibration isolation in the region of 100–200 Hz and around 24 dB in the region of 0–200 Hz. Hence, it is of interest to examine in particular the distribution of the natural frequencies that occur in/near these ranges. The distribution of the natural frequencies that occur in the frequency region of 50–250 Hz for the baseline and the best design are shown in Fig. 8. It can be seen from Fig. 8 that the baseline structure has around 42 eigenmodes in that region, whereas the optimized structure has only 33 eigenmodes. Further, it can be seen that the optimized structure has stopbands in the frequency region considered, which are marked in Fig. 8. The largest stopband has a bandwidth of around 26 Hz.

The distribution of the natural frequencies gives an indication of one of the mechanisms employed by the optimized structure to filter vibrations. Essentially, the highly irregular geometry of the structure leads to the creation of zones in the frequency region where no modes occur, which are referred to in the periodic structures literature as stopbands. This is expected to be one of the factors enabling the optimized structure to block vibrations across the frequency region considered.

The forced response of the optimized structure in Fig. 5 is next compared with its periodic counterpart in the frequency region of 110–200 Hz. Figure 9 compares the deformation pattern of the optimized structure with the baseline periodic structure. It can be seen that the optimized structure shows very low response levels

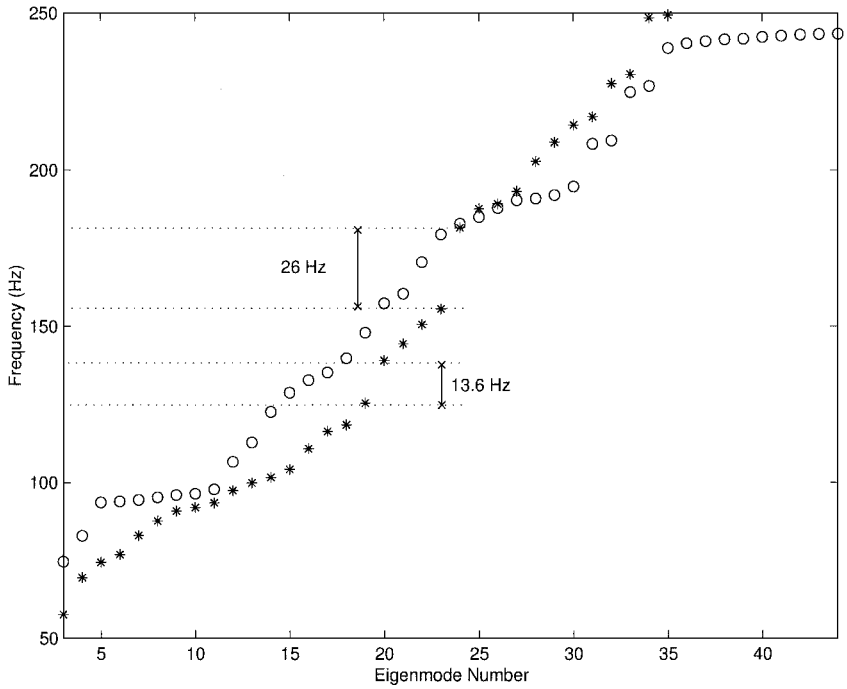

Fig. 8 Distribution of natural frequencies in the region of 50–250 Hz for the baseline and the optimized structure: ○, baseline structure; and ∗, optimized structure.

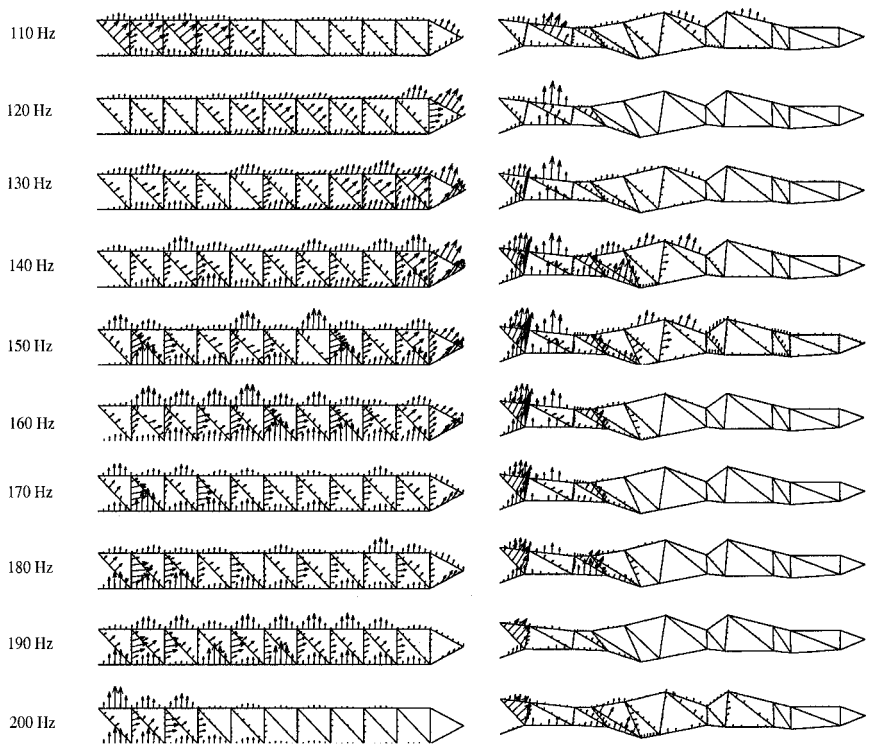

Fig. 9 Comparison of forced response behavior of the baseline and the optimized structure for excitation frequencies from 110 to 200 Hz.

at the point of excitation and the point where vibration isolation is achieved. For the baseline periodic structure, the response appears to extend throughout the length for all of the frequencies considered. In contrast, the maximum deformation levels for the optimized structure are seen to occur closer to the cantilevered end. In the frequency region of 110–200 Hz, the deformation levels in the last five bays are negligible as compared to the first four bays.

The forced response characteristics suggest that the low level of vibration transmission in the optimized structure is achieved via the reduction of displacement levels at the point of excitation, which leads to reduction in the vibrational energy input and localization of the response close to the point of excitation.

IX. Conclusions

A computational framework for the geometric redesign of flexible space structures to achieve passive vibration suppression is presented. This framework combines approximate dynamic reanalysis techniques with an AMMF developed for CGAs. The performance of the coevolutionary search strategy is compared with a conventional GA and a BFGS algorithm. The results indicate that the dynamic-stiffness-based approximation methods give better performance as compared to the modal approximation method. In particular, the use of the second-order direct frequency-response approximation method within the coevolutionary framework leads to significantly better designs as compared to the other optimization strategies considered. These results are very encouraging and suggest the applicability of the present framework to design optimization on a limited computational budget.

It is clear that significant vibration isolation of the order of 50 dB can be achieved over a 100-Hz bandwidth via passive means alone. Note that this performance was achieved with a simultaneous decrease in the structural weight of the order of 6%. Further, the optimized designs do not show any significant increase in the vibration response at frequencies that are not considered in the optimization formulation.

Studies on the free- and forced-vibration response of an optimized structure have been presented to gain insights into the mechanisms involved in the vibration filtering capability. The trends observed from the numerical studies suggest that the optimized structure intrinsically filters vibrations in the frequency bandwidth considered via three mechanisms: 1) creation of stopbands in the frequency region where no modes occur; 2) reduction of vibration amplitude at the point of excitation, which leads to reduction in the vibrational energy input; and 3) localized mode shapes, which cause vibrations to be confined near the point of excitation. More detailed studies, including robustness analysis of the optimal design have been presented in Ref. 24.

Note that in the design problem taken up only the vibration suppression level is considered in the performance index. When designing space structures for practical applications such as space interferometry missions, one needs to take into account multidisciplinary concerns from the disciplines of structural statics and dynamics, thermal analysis, active control, and optics. Hence, a practical design methodology should be multidisciplinary in nature and should rationally balance the concerns of the various disciplines. Addressing these issues for optimal synthesis of large nonperiodic space structures with enhanced vibration rejection capability is a challenging area for future research.

Acknowledgment

This research was supported by a grant from the Faculty of Engineering and Applied Sciences at the University of Southampton.

References

[1]Rosen, R., and Johnston, G. I., "Advanced Technologies to Support Earth Orbiting Systems," International Astronautical Federation, Paper IAF-92-0751, Aug.–Sept. 1992.

[2]Maghami, P. G., Gupta, S., Elliot, K. B., Joshi, S. M., and Walz, J. E., "Experimental Validation of an Integrated Controls-Structures Design Methodology for a Class of Flexible Space Structures," NASA TP-3462, Nov. 1994.

[3]Maghami, P. G., Joshi, S. M., and Armstrong, E. S., "An Optimization-Based Integrated Controls-Structures Design Methodology for Flexible Space Structures," NASA TP-3283, Jan. 1993.

[4]Junkins, J. L. (ed.), *Mechanics and Control of Large Flexible Space Structures*, Vol. 129, Progress in Astronautics and Aeronautics, AIAA, Washington, DC, 1990.

[5]Keane, A. J., "Passive Vibration Control via Unusual Geometries: The Application of Genetic Algorithm Optimization to Structural Design," *Journal of Sound and Vibration*, Vol. 185, No. 3, 1995, pp. 441–453.

[6]Keane, A. J., and Bright, A. P., "Passive Vibration Control via Unusual Geometries: Experiments on Model Aerospace Structures," *Journal of Sound and Vibration*, Vol. 190, No. 4, 1996, pp. 713–719.

[7]Langley, R. S., "Wave Transmission Through One-Dimensional Near Periodic Structures: Optimum and Random Disorder," *Journal of Sound and Vibration*, Vol. 188, No. 5, 1995, pp. 637–657.

[8]Langley, R. S., Bardell, N. S., and Loasby, P. M., "The Optimal Design of Near-Periodic Structures to Reduce Vibration Transmission and Stress Levels," *Journal of Sound and Vibration*, Vol. 207, No. 5, 1997, pp. 627–646.

[9]Keane, A. J., "Experiences with Optimizers in Structural Design," *Proceedings of the Conference on Adaptive Computing in Engineering Design and Control*, edited by I. C. Parmee, Univ. of Plymouth, Plymouth, England, U.K., 1994, pp. 14–27.

[10]Mead, D. J., "Wave Propagation in Continuous Periodic Structures: Research Contributions From Southampton 1964–1995," *Journal of Sound and Vibration*, Vol. 190, No. 3, 1996, pp. 495–524.

[11]Lust, S. D., Friedmann, P. P., and Bendiksen, O. O., "Free and Forced Response of Multi-Span Beams with Multi-Bay Trusses with Localized Modes," *Journal of Sound and Vibration*, Vol. 180, No. 2, 1995, pp. 313–332.

[12]Mester, S. S., and Benaroya, H., "Periodic and Near-Periodic Structures," *Shock and Vibration Digest*, Vol. 2, No. 1, 1995, pp. 69–95.

[13]Bendiksen, O. O., "Mode Localization Phenomena in Large Space Structures," *AIAA Journal*, Vol. 25, No. 9, 1987, pp. 1241–1248.

[14]Keane, A. J., and Manohar, C. S., "Energy Flow Variability in a Pair of Coupled Stochastic Rods," *Journal of Sound and Vibration*, Vol. 168, No. 2, 1993, pp. 253–284.

[15]Castanier, M. P., and Pierre, C., "Investigation of the Combined Effects of Intentional and Random Mistuning on the Forced Response of Bladed Disks," AIAA Paper 98-3720, 1998.

[16]Noor, A. K., "Recent Advances and Applications of Reduction Methods," *Applied Mechanics Reviews*, Vol. 47, No. 5, 1994, pp. 125–146.

[17]Nair, P. B., Keane, A. J., and Langley, R. S., "Improved First-Order Approximation of Eigenvalues and Eigenvectors," *AIAA Journal*, Vol. 36, No. 9, 1998, pp. 1721–1727.

[18]Murthy, D. V., and Haftka, R. T., "Approximations to Eigenvalues of Modified General Matrices," *Computers and Structures*, Vol. 29, No. 5, 1988, pp. 903–917.

[19]Eldred, M. S., Lerner, P. B., and Anderson, W. J., "Higher-Order Eigenpair Perturbations," *AIAA Journal*, Vol. 30, No. 7, 1992, pp. 1870–1876.

[20]Bishop, C. M., *Neural Networks for Pattern Recognition*, Oxford Univ. Press, Oxford, 1995, pp. 187–189.

[21]Zhang, D. W., and Wei, F. S., "Structural Eigenderivative Analysis Using Practical and Simplified Dynamic Flexibility Method," *AIAA Journal*, Vol. 37, No. 7, 1999, pp. 865–873.

[22]Akgun, M., "New Family of Modal Methods for Computing Eigenvector Derivatives," *AIAA Journal*, Vol. 32, No. 2, 1994, pp. 379–386.

[23]Kirsch, U., "Reduced Basis Approximation of Structural Displacements for Optimal Design," *AIAA Journal*, Vol. 29, No. 10, 1991, pp. 1751–1758.

[24]Nair, P. B., "Design Optimization of Flexible Space Structures for Passive Vibration Suppression," Ph.D. Dissertation, Computational Engineering and Design Center, School of Engineering Sciences, Univ. of Southampton, Southampton, England, U.K., Jan. 2000.

[25]Nair, P. B., Keane, A. J., and Shimpi, R. P., "Combining Approximation Concepts With Genetic Algorithm-Based Structural Optimization Procedures," AIAA Paper 98-1912, 1998.

[26]Hajela, P., "Nongradient Methods in Multidisciplinary Design Optimization: Status and Potential," *Journal of Aircraft*, Vol. 36, No. 1, 1999, pp. 255–265.

[27]Potter, M. A., "The Design and Analysis of a Computational Model of Cooperative Coevolution," Ph.D. Dissertation, Dept. of Computer Science, George Mason Univ., Fairfax, VA, 1997.

[28]Goldberg, D. E., *Genetic Algorithms in Search, Optimization and Machine Learning*, Addison–Wesley, Cambridge, MA, 1989.

[29]Zhu, C., Byrd, R. H., Lu, P., and Nocedal, J., "L-BFGS-B: FORTRAN Subroutines for Large-Scale Bound Constrained Optimization," *ACM Transactions on Mathematical Software*, Vol. 23, No. 4, 1997, pp. 550–560.

A. Messac
Associate Editor